ELSEVIER

Biochimica et Biophysica Acta 1192 (1994) 79–87

BBA Biochimica et Biophysica Acta

Voltage- and Ca^{2+}-dependence of the K^+ channel in the vacuolar membrane of *Chenopodium rubrum* L. suspension cells

Frank Werner Reifarth [a], Thomas Weiser [b], Friedrich-Wilhelm Bentrup [c,*]

[a] *Institut für Tierphysiologie der Justus-Liebig-Universität, Wartweg 95, D-35392 Giessen, Germany*
[b] *ZNS-Pharmakologie, Boehringer Ingelheim KG, D-55216 Ingelheim (Rhein), Germany*
[c] *Institut für Pflanzenphysiologie der Universität, Hellbrunnerstrasse 34, A-5020 Salzburg, Austria*

(Received 3 September 1993; revised manuscript received 15 December 1993)

Abstract

Voltage- and Ca^{2+}-dependence of the slow-activating SV-K^+ channel in the vacuolar membrane of *Chenopodium rubrum* suspension cells has been analyzed using the patch clamp technique in the vacuole-attached, outside-out and whole-vacuolar configuration. Patch-pipette perfusion was applied to measure Ca^{2+} dependence of single channels in the attached-configuration. Using the PCLAMP-software (Axon Instruments), an algorithm was developed to extract reliable individual channel data from multi-channel activity records, including open probability, mean open and closed times, as well as time constants for open and closed distributions. The channel conductance of the major open state was about 83 pS (seal resistance > 8 GΩ) at 30 mV (transmembrane voltage V_m, vacuole negative), and symmetrical 100 mM KCl. The channel exhibited a strong voltage- and a weak Ca^{2+}-activation: increasing V_m from 40 to 100 mV is equivalent to a Ca^{2+} concentration change from 10^{-7} to 10^{-4} M. Mean open probabilities at $V_m = 30$ mV were 0.03 with 1 μM and 0.09 with 100 μM Ca^{2+}. Mean open times were approx. 7 ms, and almost independent of both, voltage and Ca^{2+}. Mean closed times, however, varied in a strongly voltage- and Ca^{2+}-dependent manner, e.g., at $V_m = 30$ mV dropped from 205 to 67 ms, if Ca^{2+} was raised from 10^{-6} to 10^{-4} M. Open and closed distributions of events within bursts could be fitted by the sum of two exponentials with time constants between 0.3 and 11 ms.

Key words: Potassium ion channel, SV type; Calcium ion dependence; Voltage dependence; Multichannel analysis; Perfusion pipette; Vacuolar membrane; Tonoplast; (*C. rubrum*)

1. Introduction

Weakly K^+-selective channels with slow activation kinetics (SV-type) dominate in the vacuolar membrane (tonoplast) of higher plants including *Chenopodium rubrum* [1–4]. Conductance and pharmacology particularly of the *Chenopodium* SV-channel corresponds to the maxi-K^+ channels of some animal tissues [2–5]. Many vacuolar K^+ channels are strongly voltage-dependent outward rectifier, weakly cation selective, and occasionally Ca^{2+}-sensitive [6–11]. Ca^{2+}-activated animal K^+ channels, on the other hand, generally display complex kinetics with substates, diverse open and closed constants and burst behavior [13–16]. Although in recent years Ca^{2+} dependence and kinetics of animal K^+ channels have been extensively described [14–21], only few authors reported details of Ca^{2+} dependence or channel kinetics in plants [8,9,12,47]. Recently, we have presented evidence that calmodulin might mediate the effect of cytosolic Ca^{2+} upon SV-channel activity in the tonoplast of *Chenopodium* [22]. The aim of this study was to quantify the voltage and Ca^{2+}-dependence of the SV-K^+ channel on the basis of whole-vacuole and single-channel measurements.

A major problem of so-called single-channel recordings from plant membranes seems to arise from the considerable number of active channels in a given patch and a quick channel 'run down' during measurements [23,24]. Using the patch-clamp technique, we therefore investigated first macroscopic properties of K^+ channels in suspension cells of *Chenopodium*

* Corresponding author. Fax: +43 662 80445010. E-mail: bentrup·sb835.edvz.sbg.ac.at.

Abbreviations: P_o, t_o, t_c, channel's mean open probability, mean open and closed time, respectively; N, channel number; $E_{(L)}$, number of events of a current level L; V_m, transmembrane voltage.

SSDI 0005-2736(94)00022-H

rubrum with regard to synergism of voltage- and Ca^{2+}-activation in the whole-vacuolar configuration. Secondly, we used a method to perfuse the patch pipette during recording. Thus in vacuole-attached configuration a small patch with only few channels could be exposed to different Ca^{2+} concentrations on the cytosolic side of the patch. Our data analysis, outlined below, enabled calculation of microscopic single-channel kinetics from multiple-channel recordings, i.e., open probabilities, open and closed distributions and time constants, as well as mean open and closed times as a function of both voltage and cytosolic Ca^{2+} activity.

2. Materials and methods

Media. The reference solution contained 100 mM KCl, 2 mM $MgCl_2$, 400 mM mannitol, 100 μM $CaCl_2$ buffered with 80 μM EGTA (pH 7.2) and was buffered with 5 mM Tris-Mes. Total and free Ca^{2+} and EGTA of the test solutions were calculated according to [25,26]. Solutions contained each $\leqslant$ 10, 10, 50, 100, $\geqslant$ 100 μM Ca^{2+} with 40, 80, 80, 80, 1000 μM EGTA, respectively. Different Ca^{2+} concentrations were applied to the tonoplast during 'vacuole-attached' measurements by perfusion of the pipette solution, or during 'outside-out' and 'whole-vacuolar' measurements by chamber perfusion. Channel selectivity was investigated with 20 mM KCl (560 mM mannitol) in the pipette and 100 mM KCl (400 mM mannitol) in the chamber, respectively. Solutions were filtered (0.2 μm). All chemicals came from Sigma.

Vacuoles. Most experiments have been carried out on vacuoles isolated from heterotrophically grown, few from photoautotrophically grown cell suspensions derived from *Chenopodium rubrum*. For details see Ref. [27].

Patch clamp set-up. The general set-up was described previously [4]. Control of the test medium at the cytosolic side in the vacuole-attached mode was achieved by perfusion of the patch pipette. For this purpose, the suction pipette holder [28] was used without sliding shield. A drill hole behind the suction outlet enabled the installation of a small teflon tube (outer diameter of 0.5 mm) along the teflon coated electrode. Plasticine ensured airtight connection between the pipette holder and the tube. The tube was connected to a peristaltic pump placed near the pipette holder and used to fill and to empty the pipette solution with < 0.5 mm/s solution movement in the pipette. To prevent shaking of the test chamber and the patched vacuole when switching pump direction during attached measurements, an 'excised-attached' configuration was used. This configuration was developed by withdrawal of the pipette from the vacuole after reaching a seal in the attached-mode. Usually the membrane then formed a small vacuolar vesicle on the pipette tip which contained enough channels to produce a calm ground line. Use of both a relatively long electrode wire and pipette improved medium mixing in the pipette. After perfusion, noise was minimized by withdrawal of the medium in the pipette until only the electrode tip was covered.

Voltage and current sign. The recent sign convention was used [48]; accordingly, the transmembrane voltage (V_m) is defined as the potential difference of cytoplasm minus vacuole. Flow of positive charge from the cytoplasm to the vacuole is termed outward current and plotted upward in all graphs. Contrary to previous definition [9] the SV-K^+ channel thus is an outward rectifier with a high conductance for outward and low conductance for inward currents. In the vacuolar vesicle-attached mode a genuine transmembrane voltage of + 20 mV (vacuole interior versus cytoplasm) was assumed as measured previously [32]. In the whole-vacuolar and outside-out mode a complete exchange of the intravacuolar with the pipette solution was assumed and thus a negative holding potential was assigned as positive V_m.

Data aquisition and frequency response. We used the PCLAMP software (Version 5.5) by Axon Instruments. To derive single-channel data from the most frequent case of a patch showing multi-channel activity, we modified the data analysis as follows. The original data recorded at 40 kHz sampling rate were low pass filtered, first with 10 kHz (EPC 7 amplifier) and twice with 1.55 kHz (eight-pol-Bessel). The frequency assigned in our results correspond to the chosen frequency f_B on the front panel of the Bessel filter. Tests of the recording system included all filters and yielded an effective system time constant of $0.46/f_B$. The data were digitized on the computer with 140 μs sampling rate.

Kinetic and mathematical modelling. Channel kinetics was approximated by a two-state (open-closed) scheme. Increased channel activity due to increased voltage or Ca^{2+} concentration then appeared as follows: (Case 1) The channel open probability rose, i.e., total open time of the prevailing conductance state extended within the total time of analysis. (Case 2) The channel conductance increased. The majority of measured open events turned out to represent Case 1. Therefore, the following equations address this latter case.

3. Results

3.1. Single-channel data

Ca^{2+} dependence of single-channel activity was measured on vacuoles of heterotrophic *Chenopodium*

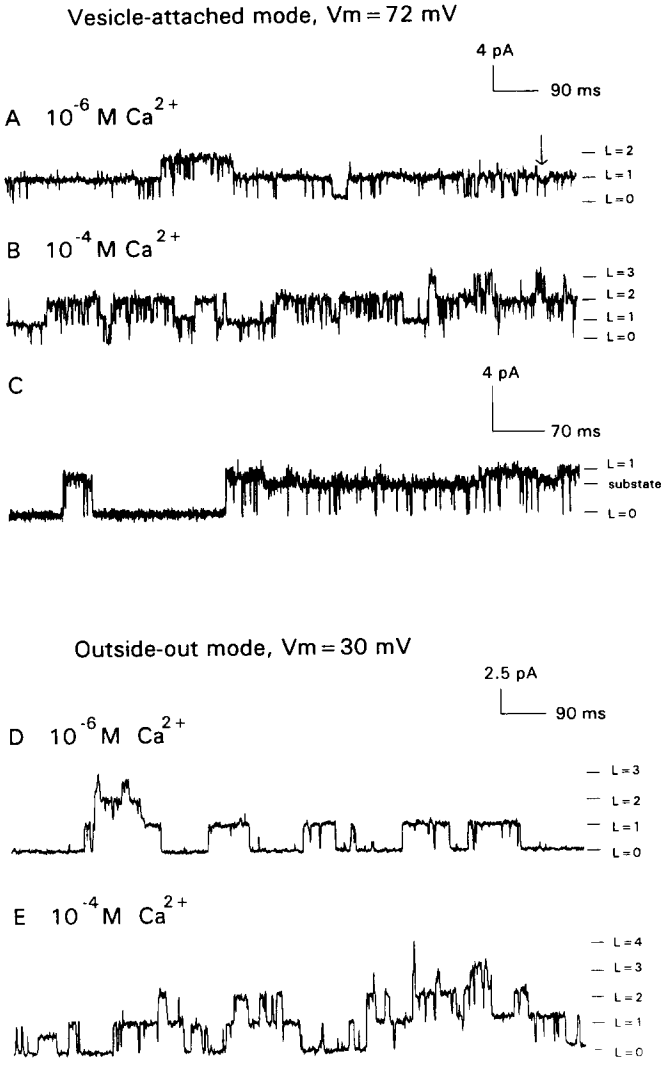

Fig. 1. Single-channel currents measured in the vacuolar vesicle-attached and outside-out mode, respectively. Indicated Ca^{2+} concentrations refer to the pipette in (A) and (B), and to the bath in (D) and (E), respectively. In (A) and (B), the predominant current amplitude is 4.2 pA. An arrow marks a smaller amplitude of 3.7 pA in trace (A), details of this substate are shown in (C). In (D) and (E) the most frequent current amplitude is 2.5 pA. Note increased channel activity in (B) versus (A) and in (E) versus (D), respectively.

rubrum cell suspensions in symmetrical 100 mM KCl solutions. Ca^{2+} concentrations were changed from 10^{-6} to 10^{-4} M on the Ca^{2+}-sensitive (cytosolic) side of the channels, and transmembrane voltages kept constant.

Calculations of single-channel kinetics were possible with up to eight channels in a given patch through extended analysis of currents data using the following procedures. Recorded currents were analysed using the PCLAMP software (FETCHAN and PSTAT):

Traces as given in Fig. 1 are subdivided in levels (L) attributed to a calculable number of active channels: $L = 0$ (groundline), $L = 1$ (sequences with only one current amplitude), $L = 2$ (sequences with two superimposed current amplitudes), $L = 3$ (sequences with three superimposed current amplitudes, $L = L_{max}$ (the maximum of visible channels in the patch open simultaneously). Each level including its superimposed sequences were analysed manually in FETCHAN (for selection of parameter edit *Event mode*). PSTAT offers in menue 'Modify/Display range or fitting parameters' with *Seed* the mean open time $t_{o(L)}$ and the number of events $E_{(L)}$ of the analyzed level L. These parameters were used in Eqs. (1)–(4).

Fig. 1 exhibits recorded sequences of channel activities. The average channel behavior within a given recording will be expressed through the channels mean open probability P_o, its mean open time t_o and mean closed time t_c, respectively, and the corresponding time constants introduced below.

The open probability of a level L was calculated as

$$P_{o(L)} = t_{o(L)} E_{(L)} / t_{total} \quad (1)$$

and the mean open probability of a single channel then is

$$P_o = N^{-1} \sum_{L=1}^{L=L_{max}} P_{o(L)} \quad (2)$$

the mean open time and mean closed time of a single channel follows simply as

$$t_o = N P_o t_{total} / \sum_{L=1}^{L=L_{max}} E_{(L)} \quad (3)$$

and

$$t_c = N(1 - P_o) t_{total} / \sum_{L=1}^{L=L_{max}} E_{(L)} \quad (4)$$

whereas t_{total} denotes the total time of analysis in FETCHAN, and N denotes the number of channels approximated through binomial distribution.

3.2. Channel number

The probability for appearance of a level in a current amplitude diagram is assumed to follow a binomial distribution [20,29,49]. This current level probabilities $P_{cur(L)}$ depended upon the number of open events of each level L and were calculated with $P_{o(L)}$ from Eq. (1). However, superimposed sequences of the respective level were excluded; i.e., $P_{cur(L)} = P_{o(L)} - P_{o(L+1)}$.

The $P_{cur(L)}$ probabilities yielded the measured binomial level distribution. This distribution was compared with the corresponding hypothetical binomial distribution.

$$P_{hyp(L)} = N!(P_{mean})^L (1 - P_{mean})^{N-L} / L!(N - L)! \quad (5)$$

whereas the mean open probability of Eq. (5) was calculated for an estimated channel number N according to

$$P_{mean} = 1 - \left(P_{cur(L=0)}\right)^{1/N} \quad (6)$$

with the measured ground line probability

$$P_{cur(L=0)} = 1 - \sum_{L=1}^{L=L_{max}} P_{cur(L)} \quad (7)$$

Optimal conformity of the distributions $P_{cur(L)}$ versus $P_{hyp(L)}$ was found via approximation and yielded the most confident channel number N. This number then was used in Eqs. (2)–(4).

Figs. 1A and B present single-channel currents recorded in the vacuolar vesicle-attached mode. Ca^{2+} concentration was kept constant at 10^{-4} M in the bath, but was changed in the pipette by perfusion from 10^{-6} to 10^{-4} M. The tonoplast was inverse polarized with a transmembrane voltage of 72 mV. The majority of channel amplitudes reflected a current of 4.2 pA, i.e., a conductance of 58 pS. Up to two (Fig. 1A) and three (Fig. 1B) simultaneous channel openings were visible. The binomial approximation of channel number in these measurement revealed three channels in Figs. 1A and 1B. A frequently observed substate at $V_m = 72$ mV is shown in Fig. 1C. Data were filtered at 1550 Hz.

Single-channel currents in the outside-out configuration are shown in Figs. 1D and 1E. During measurements Ca^{2+} concentration in the pipette and transmembrane voltage was kept constant at 10^{-4} M and 30 mV, respectively. The majority of open events reflected current amplitudes of 2.5 pA and a conductance of 83 pS. In this recording mode, increasing the Ca^{2+} concentration in the bath from 10^{-6} to 10^{-4} M concerns the Ca^{2+}-sensitive (cytoplasmic) side of the channels. Binomial approximation of the channel number revealed a fast channel 'run down'. Up to four (Fig. 1E) and three channels (Fig. 1D), respectively, showed up; however, the calculated number was eight and four channels, respectively. Data were filtered at 1550 Hz.

In Table 1 representative values for P_o, t_o and t_c have been compiled. Evidently an 100-fold increase of cytosolic Ca^{2+} from 10^{-6} to 10^{-4} M raises the channel open probability P_o only by a factor of approx. 2 to 3, as does an increase of voltage from 30 to 72 mV. Secondly, P_o obviously increases through a decrease of the closed time t_c, while the channel open time t_o remains essentially unchanged.

3.3. Open and closed distribution of several channels

Probability density functions $f(t)$ were calculated with PSTAT. Distributions with more than one rate constant correspond to superimposed exponential functions [30]. The events were binned per time interval $dF(t)/dt$ using PSTAT. Analysis of multiple-channel data by PSTAT allows to estimate the time constants of several identical channels (see below).

Table 1
Mean open probability, P_o, mean open and closed times, t_o and t_c, and time constants for open and closed distributions τ_1, τ_2, abstracted from the single-channel recordings of Figs. 1 and 2 (see text)

Ca^{2+}	P_o	t_o (ms)	t_c (ms)		Time constants (ms)	
					open	closed
Vacuolar vesicle- attached mode, $V_m = 72$ mV						
10^{-6} M	0.08	10	123	τ_1	0.70	0.45
				τ_2	9.47	1.65
10^{-4} M	0.23	6	21	τ_1	0.21	0.71
				τ_2	7.42	6.35
Outside-out mode, $V_m = 30$ mV						
10^{-6} M	0.03	6	205	τ_1	0.56	0.26
				τ_2	8.42	2.88
10^{-4} M	0.09	7	67	τ_1	0.64	0.25
				τ_2	10.55	2.52

Any recording of multi-channel activity hampers the evaluation of a probabilty density function of an individual channel. Since only currents of level 1 reveal authentic channel open and closed times, current record must contain a sufficient number of open and closed intervalls of level 1 so that single-channel kinetics can be reliably derived [30]. To ensure comparability of these distributions, upper and lower histogram limits and bin sizes have been normalized: the upper limit of open distributions was set to 100 ms and of closed distribution to 10 ms, the lower limit to 0, and the bin size to 1 and 0.3 ms, respectively. The extension of superimposed exponential functions [30] applied to two similar channels with two rate constants each exhibits a distribution with four rate constants analogous to

$$f_1(t) = a_{11}k_{11}\exp(-k_{11}t) + a_{12}k_{12}\exp(-k_{12}t) + a_{21}k_{21}\exp(-k_{21}t) + a_{22}k_{22}\exp(-k_{22}t) \quad (8)$$

with k_{11} = rate constant 1 of channel 1, k_{12} = rate constant 2 of channel 1, k_{21} = rate constant 1 of channel 2, k_{22} = rate constant 2 of channel 2; the initial constants a_{nn} are defined correspondingly.

Assuming that similar channels show nearly identical rate and initial constants, Eq. (8) can be simplified with $k_1 = k_{11} = k_{21}$, $a_1 = a_{11} = a_{21}$, $k_2 = k_{12} = k_{22}$ and $a_2 = a_{12} = a_{22}$ to $f_{(2)}(t) = 2f_{(1)}(t)$ and the rate constants thus will describe the single-channel behavior, i.e., $f_2(t) = a_1\ k_1\exp(-k_1t) + a_2\ k_2\ \exp(-k_2t) = 2f_1(t)$.

These rate constants of open and closed distributions display variable channel kinetics in dependence of the given cytoplasmic Ca^{2+} concentration. Exponential approximation of distributions within burst sequences (best fit by minimizing χ^2) yielded two time

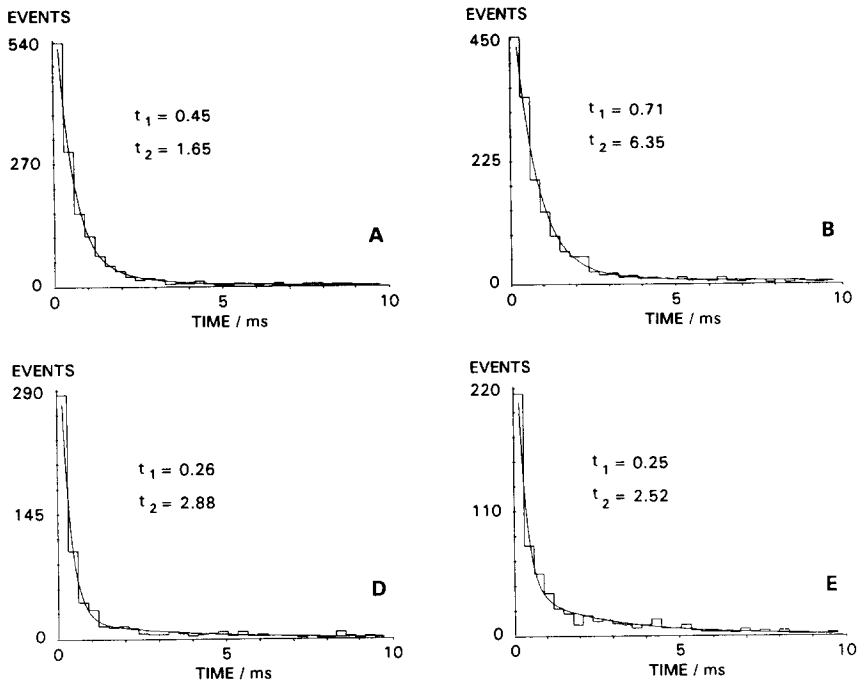

Fig. 2. 'Closed'-distribution histograms derived from intraburst channel data. Histograms and related curves (A), (B), (D) and (E) refer to the same recording modes and Ca^{2+} concentration as given in Fig. 1. Number of events have been (A): 1366, (B): 1527, (D): 580, and (E): 584. From the fitted exponential curves two time constants τ_1 and τ_2 have been derived by using PSTAT, and added to Table 1.

constants for open and closed distributions. Representative closed distributions are shown in Fig. 2. The data have been added to Table 1. Notably, Ca^{2+} concentration-dependent changes of the channel behavior may be detected independently of visible changes in channel activities of current traces; that is, increased Ca^{2+} enlarged bins in the range from 0.3 to 5 ms in closed distributions. Obviously, single-channel behavior upon a 100-fold increase in Ca^{2+} concentration revealed: (i) increased burst frequency or duration, (ii) prolonged open probability up to 3-fold and (iii) decreased mean closed times by a factor of about 3, whereas (iv) mean open times remained essentially constant.

3.4. Whole-vacuole current data

Voltage and Ca^{2+} dependence of the macroscopic current was measured in the whole-vacuolar mode with symmetrical KCl solutions (100 mM). During measurements the transmembrane voltage was changed stepwise from -100 mV to $+100$ mV; subsequently, the Ca^{2+} concentration of the bath was stepped up from 10^{-9} M to 10^{-2} M.

Analysis of whole vacuolar currents by SV-K^+ channels were performed with CLAMPEX, CLAMPAN and CLAMPFIT in the range from $V_m = -100$ mV to $+100$ mV with 20 mV steps. Outward currents at the onset of the reverse polarized test impulse prevented the calculation of the seal resistance, especially of recordings with Ca^{2+} concentrations > 100 μM (Fig. 3). Consequently, the seal resistance was estimated during neglegibly small inward currents at the end of the polarizing test impulse and subtracted from gross outward currents to obtain the net outward currents in Fig. 4. Directly after application of the nega-

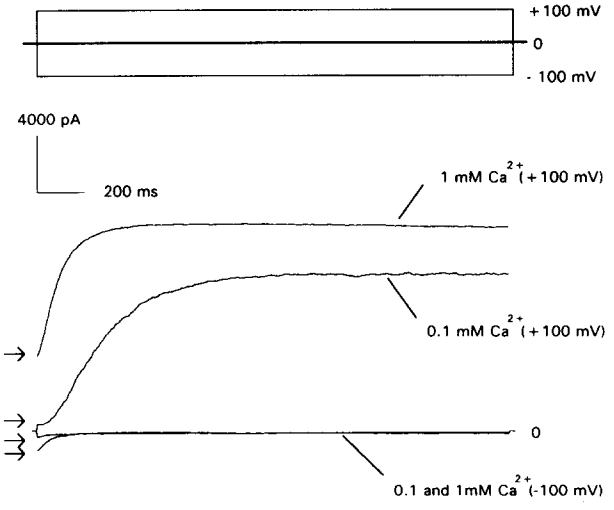

Fig. 3. Kinetics of the slow-activating clamp current in the whole-vacuolar mode ($V_m = -100$ mV, inward current, and $V_m = +100$ mV, outward current). Bath solution with 10^{-4} and 10^{-2} M Ca^{2+} as indicated. Note difference in steady-state current. Arrows indicate the onset of the vacuolar response to -100 and $+100$ mV, respectively, at $t = 2$ ms.

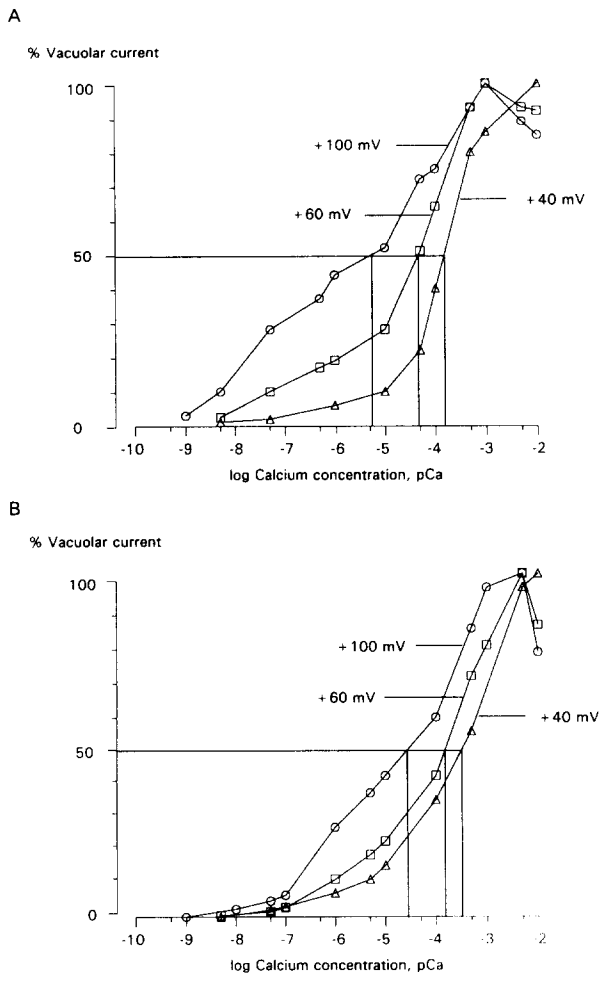

Fig. 4. Voltage- and Ca^{2+}-dependence of vacuolar currents from (A) photoautotrophically, and (B) heterotrophically grown *Chenopodium rubrum* suspension cells. The curves reflect for the indicated transmembrane voltages K^+ channel activation in the range from 10^{-9} to 10^{-2} M Ca^{2+}. Vacuolar currents are normalized; 100% denotes the maximum observed current at a given transmembrane voltage (+40, +60, +100 mV), i.e., (A) 190, 630, 1980 pA, and (B) 920, 2650, 6870 pA, respectively.

tive voltage step an about 15-fold higher current as the leak current is shown by Fig. 3. Concentrations > 1 mM Ca^{2+} seem to prevent the closure of many channels due to zero transmembrane voltage, and facilitate outward currents following the onset of the reverse polarizing test impulse; see arrows in Fig. 3.

Analysis of current–time relationships as shown in Fig. 3 delivered the following channel characteristics: (i) slow vacuolar and outward rectifying properties with a strong voltage, but a weak Ca^{2+} dependence, (ii) comparable channel activation (represented through an expanded vacuole current) was brought about by a 2.5-fold increased transmembrane voltage (40 to 100 mV) and a 1000-fold higher Ca^{2+} concentration from 10^{-7} to 10^{-4} M.

To demonstrate the effect of different transmembrane voltages on the Ca^{2+} dependence of the channels, a graph $I_{vac} = f(\lg[Ca^{2+}])$ was calculated from current-time relationships for three transmembrane voltages (Fig. 4). Figure 4A refers to photoautotrophically and Fig. 4B to vacuoles from heterotrophically grown suspension cells of *Chenopodium rubrum*. Evidently both cell cultures have similar SV-K^+ channel properties. All currents of these figures were normalized to I(100%) corresponding to the maximum vacuole currents obtained from the indicated transmembrane voltages of 40, 60 and 100 mV. At a low voltage (40 mV) curves are sigmoidal; higher voltages (60 mV and 100 mV) obviously caused apparent outward current inhibition above 10^{-3} M Ca^{2+}. Ca^{2+} concentrations for half maximum vacuolar currents and channel activation, respectively, are indicated. Maximum curve slope is visible by half-maximal outward current values at steady-state Ca^{2+} concentrations outside the physiological range (> 10^{-4} M).

4. Discussion

The kinetic data of the major Ca^{2+}- and voltage-dependent SV-K^+ channel in the tonoplast of *Chenopodium rubrum* suspension cells presented by this study, rely upon refinement of two methods. Firstly, pipette perfusion allows exchange of test media on small patches obtained with a correspondingly fine pipetted on the wanted, i.e., in this case the cytosolic side; hence application of test media may be more or less independent of the recording configuration [53,54]. This technical advantage considerably raised the number of valid single-channel recordings. Secondly, we think that the above introduced evaluation procedure provides a straightforward and satisfactorily reliable analysis of individual channel kinetics from multiple-channel patches.

4.1. Voltage and Ca^{2+}-dependence

Voltage- and Ca^{2+}-controlled K^+ channels are well known from animal tissues [13,14,16–21], but only few reports are available for such channels and their kinetic properties in plants [9,12,31,47]. We have recently reported on the pharmacology and the probable involvement of calmodulin in the SV-K^+ channel of *Chenopodium rubrum* [4,5,22]. The present study provides quantitative details of the voltage- and Ca^{2+}-dependence of this SV-K^+ channel derived from multiple-channel patch analysis and whole vacuolar recordings.

Patches exhibiting electrical activity of just one channel at a time over a satisfactory span of, say, 15 min have not been observed. Multiple-channel recordings are easier to obtain, but more complicated in terms of individual channel kinetics. Although various

methods exist to solve the mathematical problems of analyzing multiple-channel activity [20,32–34,46,50,55], the obstacle of usually instable activities and low open probabilities of the SV-channel (about 0.1) prompted us to develop a simple analytical procedure applicable to multiple-channel data. The algorithm introduced above allows data evaluation to reveal open probabilities as low as 0.03 from only 500 events with less than 20% failure; the algorithm is compatible with the PCLAMP software. Consequently each level of a channel current was separately analysed. Level-data were used to approximate the channel number within a given patch, to calculate mean open and closed probabilities, and also time constants of an individual channel. The analytical procedure was based on following assumptions: only one type of channel is active in a given patch, having only one conductance state, and operate independently. Although current traces exhibited different amplitudes (Fig. 1) and clustered openings due to multiple-channel activity [16,30], the majority of current sequences satisfactorily met these assumptions, because the majority of channel openings showed a constant current amplitude, and because current levels could be described by the binomial distribution.

Channel kinetics have been simplified to a two state (open-closed) scheme. Analysis of the open-flickering-shut state would have required an enhanced time resolution [51] which, however, was limited by the increased noise from the perfusion pipette and therefore was omitted. Intraburst open and closed distributions were approximated with PSTAT by minimizing χ^2 values. Close fit was only achievable with two exponentials ($\chi^2 < 200$), whereas a one-exponential fit gave $\chi^2 > 2 \cdot 10^6$ and therefore is not presented. Closed distributions measured with 72 mV (Figs. 2A, 2B) delivered an enlarged first time constant compared to data at 30 mV (Figs. 2C, 2D) which might result from the voltage dependent block of divalent cations, as Mg^{2+} or Ca^{2+} [12,16,31,40,54]. Corresponding to these findings open distributions at 72 mV and 10^{-4} M Ca^{2+} showed shortened time constants (Table 1).

Channel recordings with less than eight channels frequently displayed a fast channel 'run down', i.e., channel currents disappear and channel kinetics altered within the first 5 min after the gigaseal has been formed; similar observations have been reported, for instance, by [23,24,35]. Yet we needed at least 15 min for two changes of pipette medium during an attached measurement and for recording a sufficient number of events from identical channels, e.g., for changing the pipette solution from 10^{-4} to 10^{-6}, and back to 10^{-4} M Ca^{2+}. Consequently, we estimated the mean channel number using the binomial distribution. Some help against channel 'run down' of single-channel patch preparations may come from application of sulfhydryl-reductants [23,36]. By contrast, whole-vacuolar measurements yielded stable channel behaviour for up to 2 h.

The Ca^{2+} dependent SV-K^+ channels of *Chenopodium rubrum* vacuoles displayed a channel conduction of 83 pS in symmetrical 100 mM KCl at 30 mV transmembrane voltages across a seal resistance of about 8 GΩ. This conductance seems typical for large vacuolar channels [3] and fairly compares with the conductance of Ca^{2+}-dependent maxi-K^+ channel in animal systems [13,14,17–19]. The *Chenopodium* channel resembles the quoted class of animal channels also regarding bursts and substates [13–15,17], and notably of pharmacology [4,5,14,15].

Transmembrane voltage and Ca^{2+} concentration control the open probability of the *Chenopodium* K^+ channel essentially through the mean closed time t_c (Table 1); a comparable kinetic feature is known from K^+ channels in the plasma membrane of *Arabidopsis* [36]. On the other hand, Ca^{2+} -activated K^+ channels in cultured rat muscle [13] show a relatively high Ca^{2+} sensitivity: a 3-fold increased Ca^{2+} changed channel open probability from 0.1 to 0.9, whereas the present *Chenopodium* channel responds to a 100-fold change in Ca^{2+} with change in open probability from 0.03 to 0.09 only (Table 1); see below.

We deemed it instructive to test the macroscopic properties of both, photoautotrophically and heterotrophically grown suspension cells; the former essentially represent the photosynthetically active mesophyll tissue of the green leaf and the latter the storage tissue of a stem or root within the differentiated plant. The whole-vacuolar data confirm for both cell lines the reported Ca^{2+} dependence of the SV-K^+ channel from sugar beet vacuoles [9]; additionally, in Fig. 4 we show the strong voltage dependence. Only the cytosolic side displayed a, in fact small, Ca^{2+} sensitivity of channel activation. Half-maximum whole vacuolar currents were attainable with Ca^{2+} concentrations of approx. 0.1 mM. Comparison of these value with the observed maximum cytoplasmic free Ca^{2+} concentration < 0.4 μM [37–39] are consistent with the hypothesis that calmodulin might mediate the control of the channel by the cytoplasmic free Ca^{2+} [22]. Curves in Fig. 4 appear sigmoid only for low activation voltages, $V_m = 40$ mV. Saturating and inhibiting effects by Ca^{2+} concentrations $> 10^{-4}$ M seen here are also reported for animal and plant K^+ channels [12,16,18,19,47]. Presumably, Ca^{2+} and other bivalent ions (e.g., Ba^{2+}) can be pressed, especially by transmembrane voltages > 50 mV, into the channel, and then might block the entry of other ions. Penetration of such hydrated ions would be reasonable for high conductance channels which pass more than one monovalent ion simultaneously, i.e., have corresponding large diameters [12,14,16,40–43,47].

Table 2
Percent whole vacuolar currents derived from interpolation of current-time relations in the voltage range 20 to 40 and 60 to 80 mV, respectively, and single-channel open probability P_o abstracted from Table 1 for given transmembrane voltages and Ca^{2+} concentrations

	Vacuolar current		Open probability P_o	
	30 mV	70 mV	30 mV	72 mV
10^{-6} M Ca^{2+}	5%	18%	0.03	0.08
10^{-4} M Ca^{2+}	24%	55%	0.09	0.23

Opening of the rectifying K^+- channels of the present study completely depends upon a sufficiently reverse polarization, because the mean steady-state voltage across the tonoplast is about + 20 mV (vacuolar interior versus cytoplasm) [27]; however, locally reverse polarization through Ca^{2+} channels conducting vacuolar Ca^{2+} into the cytoplasm is conceivable [38]; thus local reverse polarization of up to $V_m = 100$ mV and the increased Ca^{2+} concentration could elicit massive opening of surrounding K^+ channels [39] and solve this discrepancy. Similar examples were reported for channels in the plasmalemma [3,11] as well as in human erythrocytes [52]. Vacuolar channels seem also to be regulated by cytoplasmic chloride [55].

4.2. Whole vacuolar versus single-channel data

Whole vacuolar- and single-channel data obtained at nearly identical V_m values exhibit comparable voltage- and Ca^{2+}-dependence (Table 2). Increased Ca^{2+} concentrations caused prolonged open probabilities of single channels (Table 1) and enlarged vacuolar currents during whole vacuolar measurements (Fig. 4). Table 2 shows that comparable channel activation is brought about by 100-fold increased Ca^{2+} concentration versus 2.3-fold increased voltage. Furthermore, 100-fold increased Ca^{2+} activated the channels about 3–4-fold at low, and about 2–3-fold at high V_m. This correlation confirms our notion that the whole vacuolar currents indeed are predominantly generated by the K^+-channel of the SV-type emerging from the patch data. However, provided that channels of whole vacuolar measurements delivered open probabilities up to 1, channel activities during single-channel recordings seems to be reduced about 2-fold in comparison to whole vacuolar measurements (Table 2).

4.3. Ion selectivity

A conventional tail current analysis was carried out in the outside-out mode with asymetrical KCl solutions, i.e., 20 mM in the pipette and 100 mM in the bath (data not shown). The current-voltage-relations showed a reversal potential of 13 mV. According to the Goldman equation a permeability ratio of P_K/P_{Cl} of 2.2 was calculated. A similarly limited selectivity for monovalent cations, including an appreciable anion conductance, has been reported for tonoplast-bound SV channels from other plants [3,6,7,44,45].

Acknowledgements

We are grateful to Petra Stutz for rearing the cell cultures. This work was supported by the Deutsche Forschungsgemeinschaft (Grant Be 466/21) and by the Bundesminister für Forschung und Technologie, Bonn.

References

[1] Hedrich, R., Barbier-Brygoo, H., Felle, H., Flügge, U.I., Lüttge, U., Maat-huis, F.J.M., Marx, S., Prins, H.B.A., Raschke, K., Schnabl, H., Schroeder, J.I., Struve, I., Taiz, L. and Ziegler, P. (1988) Bot. Acta 101, 7–13.
[2] Tester, M. (1990) New Phytol. 114, 305–340.
[3] Weiser, T. and Bentrup, F.-W. (1990) FEBS Lett. 277, 220–222.
[4] Weiser, T. and Bentrup, F.-W. (1991) Biochim. Biophys. Acta 1066, 109–110.
[5] Weiser, T. and Bentrup, F.-W. (1993) J. Membr. Biol. 136, 43–54.
[6] Hedrich, R., Flügge, U.I. and Fernandez, J.M. (1986) FEBS Lett. 204, 228–232.
[7] Coyaud, L., Kurkdjian, A., Kado, R. and Hedrich, R. (1987) Biochim. Biophys. Acta 902, 263–268.
[8] Kolb, H.-A., Köhler, K. and Martinoia E. (1987) J. Membr. Biol. 95, 163–169.
[9] Hedrich, R. and Neher, E. (1987) Nature 329, 833–835.
[10] Hedrich, R. and Kurkdjian, A. (1988) EMBO J. 7, 3661–3666.
[11] Bentrup, F.-W. (1990) Physiol. Plant. 79, 705–711.
[12] Laver, D.R. and Walker, N.A. (1991) J. Membr. Biol. 120, 131–139.
[13] Barret, J.N., Magleby, K.L. and Pallotta, B.S. (1982) J. Physiol. 331, 211–230.
[14] Schlatter, E., Bleich, M., Hirsch, J., Markstrahler, U., Fröbe, U. and Greger, R. (1993) Pflügers Arch. 422, 427–435.
[15] Lucchesi, K.J. and Moczydlowski, E. (1991) J. Gen. Physiol. 97, 1295–1319.
[16] Latorre, R. (1986) in Ion Channel Reconstitution (Miller, C., ed.), pp. 431–468, Plenum Press, New York and London.
[17] Oberhauser, A., Alvarez, O. and Latorre, R. (1988) J. Gen. Physiol. 92, 67–86.
[18] Davidson, R.M. (1993) J. Membr. Biol. 131, 81–92.
[19] Hirsch, J. Leipziger, J. Fröbe, U. and Schlatter, E. (1993) Pflügers Arch. 422, 492–498.
[20] Rae, J.L., Levis, R.A. and Eisenberg, R.S. (1988) in Ion Channels (Narahashi, T., ed.), Vol. 1, pp. 283–325, Plenum Press, New York and London.
[21] Triggle, D.J. (1990) Neurotransmissions RBI (Publ.) 6, No. 3.
[22] Weiser, T., Blum, W. and Bentrup, F.-W. (1991) Planta 185, 440–442.
[23] Bertl, A. and Slayman C.L. (1991) Plant Physiol. 96 (Suppl.), 1b.
[24] Katsuhara, M., Mimura, T. and Tazawa, M. (1991) Plant Cell Physiol. 32, 179–184.
[25] Bartfai, T. (1979) in Advances in Cyclic Nucleotide Research (Brooker, G., ed.), Vol. 10, pp. 219–241, Greengard and Robinson Raven Press, New York.

[26] Tsien, R.Y. and Ring, T.J. (1980) Biochim. Biophys. Acta 599, 623–638.
[27] Bentrup, F.-W., Gogarten-Boeckels, M., Hoffmann, B., Gogarten, J.P. and Baumann, C. (1986) Proc. Natl. Acad. Sci. USA 83, 2431–2433.
[28] Hamill, O.P., Marty, A., Neher, E., Sakmann, B. and Sigworth, F.J. (1981) Pflügers Arch. 391, 85–100.
[29] Colquhoun, D. and Hawkes, A.G. (1985) in Single Channel Recording (Sakmann, B. and Neher, E., eds.), Vol. 2, pp. 135–174, Plenum Press, New York and London.
[30] Colquhoun, D. and Sigworth, F.J. (1985) in Single Channel Recording (Sakmann, B. and Neher, E., eds.), Vol. 2, pp. 191–263, Plenum Press, New York and London.
[31] Klieber, H.G. and Gradmann, D. (1993) J. Membr. Biol. 132, 253–265.
[32] Fenwick, E.M., Marty, A. and Neher, E. (1982) J. Physiol. 331, 577–597.
[33] Jackson, M.B. (1985) Biophys. J. 47, 129–137.
[34] Frindt, G., Silver, R.B., Windhacher, E.E. and Palmer, L.G. (1993) Am. J. Physiol. 264, F565–F574.
[35] Fenwick, E.M., Marty, A. and Neher, E. (1982) J. Physiol. 331, 599–635.
[36] Spalding, E.P., Slayman, C.L., Goldsmith, M.H.M, Gradman D. and Bertl, A. (1992) Plant Physiol. 99, 96–102.
[37] Felle, H. (1988) Planta 176, 248–255.
[38] Evans, D.E., Briars, S.-A. and Williams, L.E. (1991) J. Exp. Bot. 42, 285–303.
[39] Schroeder, J.I. and Thuleau, P. (1991) Plant Cell. 3, 555–559.
[40] Laver, D.R. (1990) J. Membr. Biol. 118, 55–67.
[41] Tester, M. (1988) J. Membr. Biol. 105, 87–94.
[42] Thiel, G. and Blatt, M.R. (1991) J. Plant Physiol. 138, 326–334.
[43] Laver, D.R. (1992) J. Gen. Physiol. 100, 269–300.
[44] Maathuis, F.J.M. and Prins, H.B.A. (1990) Plant Physiol. 92, 23–28.
[45] Pantoja, O., Dainty, J. and Blumwald, E. (1990) Plant Physiol. 94, 1788–1794.
[46] Ramanan, S.V., Fan, S.F. and Brink, P.R. (1992) J. Neurosci. Methods 42, 91–103.
[47] Bertl, A., Slayman, C.L. and Gradmann, D. (1993) J. Membr. Biol. 132, 183–199.
[48] Bertl, A., Blumwald, E., Coronado, R., Eisenberg, R., Findlay, G., Gradmann, D., Hille, B., Köhler, K., Kolb, H.A., MacRobbie, E., Meissner, G., Miller, C., Neher, E., Palade, P., Pantoja. O., Sanders, D., Schroeder, J., Slayman, C.L., Spanswick, R., Walker, A. and Williams, A. (1992) Science 258, 873–874.
[49] Sachs, F., Neil, J. and Barkakati, N.(1982) Pflügers Arch. 395, 331–340.
[50] Cassola, A., Giebisch, G. and Wang, W. (1993) Am. J. Physiol. 264, F502–F509.
[51] Schultze, R. and Draber, S. (1993) J. Membr. Biol. 132, 41–52.
[52] Leinders, T., Van Kleef, R. and Vijerberg, H. (1992) Biochim. Biophys. Acta 1112, 67–74.
[53] Cull-Candy, S.G. and Parker, I. (1985) in Single Channel Recording (Sakmann, B. and Neher, E., eds.), Vol. 2, pp. 389–407, Plenum Press, New York and London.
[54] Shioya, T. Matsuda, H. and Noma, A. (1993) Pflügers Arch. 422, 427–435.
[55] Pantoja, O., Dainty, J. and Blumwald, E. (1992) J. Membr. Biol. 125, 219–229.